Int. J. Electrochem. Sci., 13 **(2018)** 1495 – 1504, doi: 10.20964/2018.02.19

International Journal of
ELECTROCHEMICAL
SCIENCE
www.electrochemsci.org

Study on Electrochemical Performance of $LiMg_{0.06}Mn_{1.94}O_4$ Synthesized by Solid-State Combustion Method

Gang Li[1,2,3], *Yue Yu*[1,2,3], *Jintao liu*[1,2,3], *Tao Feng*[1,2,3], *Miaomiao Shao*[1,2,3], *Changwei Su*[1,2,3], *Junming Guo*[1,2,3,*]

[1] Key Laboratory of Comprehensive Utilization of Mineral Resources in Ethnic Regions, Yunnan Minzu University, Kunming 650500, *PR* China
[2] Key Laboratory of Resource Clean Conversion in Ethnic Regions, Education Department of Yunnan, Yunnan Minzu University, Kunming 650500, *PR* China
[3] Joint Research Centre for International Cross-border Ethnic Regions Biomass Clean Utilization in Yunnan, Yunnan Minzu University, Kunming 650500, PR China
[*]E-mail: guojunming@tsinghua.org.cn

Received: 18 August 2017 / *Accepted:* 3 November 2017 / *Published:* 28 December 2017

Spinel $LiMg_{0.06}Mn_{1.94}O_4$ cathode materials for lithium-ion batteries were prepared by a solid-state combustion method at 500℃ in different time (1, 3, 6 and 9h). The structure and morphologies of $LiMg_{0.06}Mn_{1.94}O_4$ samples were characterized by scanning X-ray diffraction (XRD) and electron microscopy (SEM), respectively. It turned out that all samples show a single phase $LiMn_2O_4$ spinel structure with a good crystallinity. The electrochemical performances of the samples were investigated by charge-discharge cycling test and cyclic voltammetry. By means of charge-discharge cycling test, $LiMg_{0.06}Mn_{1.94}O_4$ synthesized at burning reaction time 6h had a better electrochemical performance, which presents a capacity retention rate of 81.25% after 500th cycles at 1C (1C=148 mAh/g) with initial discharge capacity of 101.9 mAh/g. Simultaneously, $LiMg_{0.06}Mn_{1.94}O_4$ prepared at 6h exhibits the lowest apparent activation energy than other samples, which indicated that Li^+ with a higher diffusion rate in the lattice, and show a better electrochemical performance.

Keywords: Solid-state combustion synthesis, Mg-doped, Spinel $LiMn_2O_4$, Lithium-ion batteries(LIBs), Cathode materials

1. INTRODUCTION

Rechargeable Lithium-ion batteries has been occupied the energy supply market because they are widely used for portable energy storage, portable devices, electric vehicles(EVs). The cathode materials play a crucial role in the improvement of energy storage capacity of LIBs.[1] There are three mainstream types of cathode materials for LIBs, such as layer structure ($LiCoO_2$ and $LiNiO_2$), olivine

structure ($LiFePO_4$) and spinel structure ($LiMn_2O_4$)[2]. Among these cathode materials, spinel $LiMn_2O_4$ is still well recognized as one of the most promising cathode materials for Lithium-ion batteries[3,4] due to its low cost, good safety and environmental friendliness, and has been attracted extensively attention [5,6]. However, the large-scale application of $LiMn_2O_4$ is confined by seriously capacity decay during the prolonged electrochemical cycles[7]. Capacity attenuation of spinel $LiMn_2O_4$ results from: (1) Jahn-Teller effect in the spinel structure; (2) disproportionation reaction of manganese into the electrolyte solution[8].

The cations ions doping has been researched extensively as one of the most comprehensive and effective ways to limit the Jahn-Teller effect, and improve the structural stability of $LiMn_2O_4$ cathode material[9]. At present, metal cation doping have been widely studied, such as Al^{3+}[10], Mg^{2+}[11], Cr^{3+}[12], Ni^{2+}[13], La^{3+}[14], Nb^{5+}[15] and so on. Among these cations, Mg^{2+} has been regarded as one of the most appropriate dopants since it is eco-friendly, low-cost, resource-rich and so on. Currently, Mg-doped $LiMn_2O_4$ has been reported less. Huang et al[16]. Reported the $LiMg_{0.05}Mn_{1.95}O_4$ sample was prepared by molten-salt combustion method, which presented a remarkable cycling stability with an initial discharge specific capacity of 122.0 mAh/g and capacity retention of 86.4% after 100 cycles at 1C. Xiang et al.[17] studied the influences of reaction temperature on $LiMg_{0.08}Mn_{1.92}O_4$ cathode materials. The as-prepared sample at 600℃ exhibited excellent capacity retention rate of 98.1% after 40 cycles with an initial discharge capacity of 101.3 mAh/g at 0.2C. Besides, Zhang et al.[18] prepared $LiMg_{0.05}Mn_{1.95}O_4$ cathode materials by microwave sintering method, the sample was present a good initial discharge capacity of 122 mAh/g at 1C. Liu et al. [19] synthesized spinel $LiMg_{0.04}Mn_{1.96}O_4$ via solid-state combustion method at various combustion reaction time, results shows that the $LiMg_{0.04}Mn_{1.96}O_4$ sample calcined in 600℃ for 6h delivered better electrochemical properties, Its initial discharge capacity is 112.4 mAh/g, and the capacity retention rate was 93.0% after 40 cycles. However, the effect of the combustion time on the apparent activation energy of Mg-doped spinel $LiMn_2O_4$ has not been reported. This paper explored in detail the relationship between apparent activation energy and calcination time.

In this work, $LiMg_{0.06}Mn_{1.94}O_4$ samples were synthesized by a solid-state combustion reaction using manganese carbonate and lithium carbonate as raw materials, magnesium acetate as Mg^{2+} dopant, citric acid as fuel. The effect of reaction time on the crystal structure, morphology, electrochemical performance, its evaluated temperature performance, and the apparent activation energy of $LiMg_{0.06}Mn_{1.94}O_4$ cathode material were investigated.

2. EXPERIMENTAL

2.1 Preparation of $LiMg_{0.06}Mn_{1.94}O_4$ materials

$LiMg_{0.06}Mn_{1.94}O_4$ samples were synthesized by a citric acid-assisted solid-state combustion reaction .take advantage of absolute ethyl alcohol as medium lithium carbonate(AR, Sinopharm Chemical reagent Co, Ltd.), manganese carbonate (AR, alading) and magnesium acetate (AR, Sinopharm Chemical reagent Co., Ltd.) were weighted according to a stoichiometric ratio of 1: 1.94: 0.06(Li: Mn: Mg) with a total mixture mass of 30.0g and put it into a agate jar. Then mass fraction of

5% citric acid (AR, Sinopharm Chemical reagent Co., Ltd) as fuel, which was also dispersed in to the jar. Then, the mixture was ball-milled. The resultant mixture was powder after drying at 80℃ in an oven. Subsequently, the powder of 5.5g was put in an alumina crucible and calcined in a muffle furnace at 500℃ for different time (1, 3, 6 and 9h) in air atmosphere. After cooling naturally to ambient temperature, the black $LiMn_{1.94}Mg_{0.06}O_4$ powders were obtained.

2.2 Characterization of $LiMg_{0.06}Mn_{1.94}O_4$ materials

Characterization of the $LiMg_{0.06}Mn_{1.94}O_4$ powders was explored by X-ray diffraction (XRD, D/max-TTRIII, Japan) with CuKα radiation(λ=0.154 nm) to confirm the crystal structure and the scanning range was from 10° to 70° with 0.02° step size and scan speed was 2° min^{-1} at an operation current of 30 mA and voltage of 40 kV. Lattice parameters were obtained by means of the Jade 5.0 soft-ware. The morphology of the $LiMg_{0.06}Mn_{1.94}O_4$ samples was observed by scanning electron microscopy (SEM, QUANTA-200 America FEI Company).

2.3 Electrochemical studies of $LiMn_{1.94}Mg_{0.06}O_4$ samples

The electrode were study by roll-pressing a mixed paste of $LiMg_{0.06}Mn_{1.94}O_4$, acetylene black, and PVDF with a weight ratio of 8:1:1 in a 100mL agate jar mill filled with appropriate N-methty1-2-pyrrolidone (NMP) solvent using as binder for 1 hours and 30 minutes and then spread uniformly on an aluminum foil by using doctor-blade technique, drying in an oven at 80℃ for 4h, and lastly punched into circular disks with 16mm diameter after pressure rolling. All as-prepared cathode disks were dried at 120℃ in vacuum oven for 12 h before cell assembling. The electrolyte was 1.0 M $LiPF_6$ solved in EC/DMC (1:1 in volume). The electrochemical evaluation was performed by using CR2025 coin-type cells assembled in a dry argon-filled glove box with lithium metal as the negative electrode. A Celgard 2320-type microporous membrane was used as the separator. The cyclic performance was studied by Land electric test system CT2001A(Wuhan Jinnuo Electronics CO., LTD.) at a current density of 1 C between 3.00 and 4.50V (vs Li/Li^+). Cyclic voltammogram (CV) tests were performanced on ZAHNER Zennium IM6 Electrochemical Workstation (ZAHNER-elektrik GmbH&Co.KG, kronach, Germany) at a scanning speed of 0.05 mV S^{-1}.

3. RESULT AND DISCUSSION

3.1 Structure and Morphology

Fig.1 shows the XRD patterns of $LiMg_{0.06}Mn_{1.94}O_4$ synthesized at 500℃ for different time. All samples present the characteristic diffraction peaks of the cubic spinel $LiMn_2O_4$ with the Fd3m space group, corresponding to eight crystal planes of (111), (311), (222), (400), (331), (511), (440) and (531).

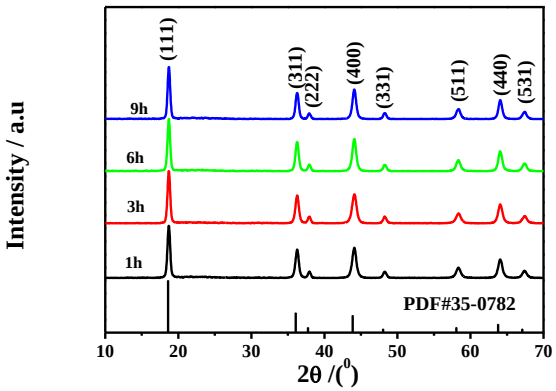

Figure 1. XRD patterns of $LiMg_{0.06}Mn_{1.94}O_4$ samples synthesized at 500℃ for different time(1h, 3h, 6h and 9h).

Table 1. The lattice parameter of $LiMg_{0.06}Mn_{1.94}O_4$ samples synthesized at 500℃ for different combustion reaction time(1h, 3h, 6h and 9h).

Combustion reaction time (h)	Lattice constant (Å)	Cell volume (Å^3)	2θ (400) peak (°)	FWHM (400) peak (°)	Crystal grain size (nm)
1h	8.2463	560.76	44.05	0.421	187
3h	8.2459	560.68	44.01	0.337	218
6h	8.2452	560.54	43.97	0.325	234
9h	8.2387	559.21	43.94	0.298	267

The characteristic peaks of the spinel $LiMn_2O_4$(JCPDS, PDF 35-0782), all as-prepared samples are single phase, which demonstrates the crystal structure of $LiMn_2O_4$ wasn't transformed after Mg-doping and combustion for different time. As can be seen from the Table 1, with the increase of the combustion reaction time, the FWHM of (400) gradually reduced. Besides, the cell parameters of the samples was decrease, which was indicated that extend the combustion time can be enhance crystallinity, and all the cell parameter was less than standard value of spinel $LiMn_2O_4$(8.427 nm), this phenomenon can be explained as follow: the Mn^{3+} is substituted by $Mg^{2+,}$ because of radius of Mg^{2+} ion (r=0.065 nm) is smaller than leads the radius of Mn^{3+}(r=0.066 nm), which lead the shrinkage of the spinel lattice[16, 20]. Furthermore, according to the Scherrer formula $D_c = 0.89\lambda / B\cos\theta$ (λ=0.154 nm, B was the FWHM, θ was the Diffraction angle of (400) Planes)[21]. It can be find that with the addition of combustion reaction time, the crystal grain size grows slightly, it shows that increasing the calcination time has an effect on the grain size, but it is not significant.

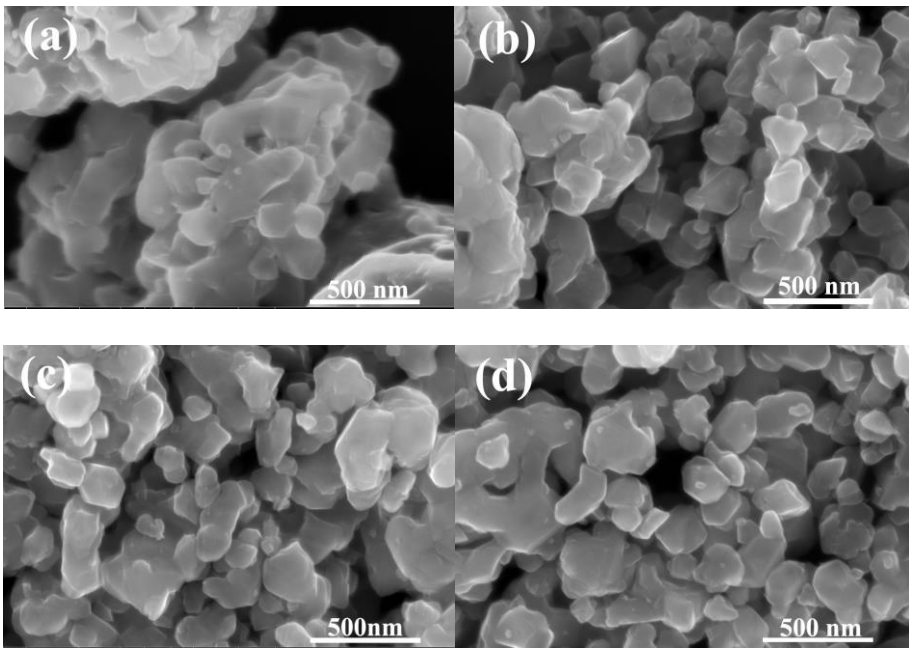

Figure 2. SEM images of $LiMg_{0.06}Mn_{1.94}O_4$ samples synthesized at 500℃ for different time. (a) 1h, (b) 3h, (c) 6h and (d) 9h

Fig.2 shows the SEM images of $LiMg_{0.06}Mn_{1.94}O_4$ calcined at 500℃ for various reaction time. It can be observed that all the samples were agglomerated, which are composed of much small crystallites. With the increase of the combustion time, the phenomenon of agglomeration gradually weakened, and the outline and boundary of truncated octahedral morphology of $LiMg_{0.06}Mn_{1.94}O_4$ become more clear, which indicated that with the addition of reaction time the crystallinity of $LiMg_{0.06}Mn_{1.94}O_4$ gradually increased. Besides, with the addition of reaction time, crystal particles gradually grow completely, the size distribution of the crystal particles gradually uniform, as can be clearly seen from Fig.2(d), the particle size of the crystal is about 200nm, this is consistent with the result obtained in Table 1.

3.5 XPS(X-ray photoelectron spectra)

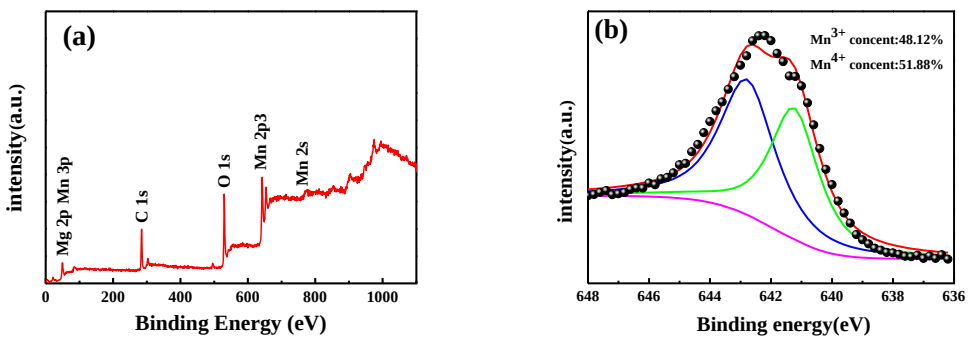

Figure 3. (a) XPS spectra of $LiMg_{0.06}Mn_{1.94}O_4$ (500℃-6h) sample, (b) fitted profiles of specific Mn $2P_{3/2}$ peak of $LiMg_{0.06}Mn_{1.94}O_4$

In order to further study the valence of manganese in $LiMg_{0.06}Mn_{1.94}O_4$, XPS analysis was characteristic to identify the surface valence of Mn of the $LiMg_{0.06}Mn_{1.94}O_4$ samples, we chose the best performance sample(500℃-6 h) for XPS analysis. There is a broad peak width located at range of 636.0 eV to 648.0 eV, which indicated that the Mn exist in more than one oxidation state. To exactly calculate the contents of Mn^{3+} and Mn^{4+}, specific Mn $2P_{3/2}$ peak of $LiMg_{0.06}Mn_{1.94}O_4$ was fitted and the result is exhibited in Fig.3(b). Wherein the content of Mn^{3+} is 48.12%, the content of Mn^{4+} is 51.88%. Theoretically, for pristine $LiMn_2O_4$, the contents of Mn^{3+} and Mn^{4+} are equal, however, for $LiMg_{0.06}Mn_{1.94}O_4$ samples, the ratio of the contents of Mn^{4+} and Mn^{3+} is 1.078, which was higher than 1, it can be demonstrated that Mg-doping can reduce the content of Mn^{3+}, and increase the average valence of Mn. Besides, because of radius of Mg^{2+} ion (r=0.065 nm) approaches the radius of Mn^{3+}(r=0.066 nm), the Mn^{3+} is substituted by Mg^{2+} in the octahedral 16d site. To balance the system valence electrons, residual Mn^{3+} in 16d sites partially convert into Mn^{4+} ions, resulting in an increase in the average valence of Mn and suppresses the Jahn-Teller effect[22, 23]. It means Mg-doped can enhance the stability of the lattice. However, the characteristic peaks of Mg can not be seen in Fig.3(a), this is due to doping amount of Mg is too little, can not be detected by the instrument.

3.2 Galvanostatic Cycling

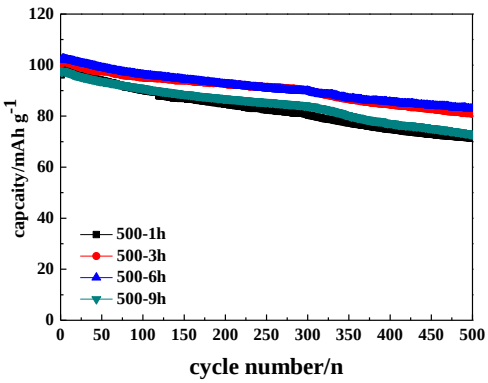

Figure 4. Cycling performance of $LiMg_{0.06}Mn_{1.94}O_4$ sample synthesized at 500℃ for different combustion reaction time(1h, 3h, 6h and 9h) between 3.0and 4.5 V at 1 C rate

Table 2. Discharge specific capacity and capacity retention of $LiMg_{0.06}Mn_{1.94}O_4$

Combustion reaction time (h)	Discharge specific capacity (mAh/g)		Capacity retentions (%)
	First cycle	500th cycle	
1	96.1	71.3	74.19
3	100.4	81	80.68
6	101.9	82.8	81.25
9	97.3	72.9	74.92

Fig.4(a) and Table 2. displays cycling performance of $LiMg_{0.06}Mn_{1.94}O_4$ samples (1, 3, 6 and 9h) at 1C rate in the voltage range of 3.00-4.50 V(vs.Li/Li^+). The $LiMg_{0.06}Mn_{1.94}O_4$ calcined for 6h shows the highest initial discharge specific capacity of 101.9 mAh/g. Meanwhile, The $LiMg_{0.06}Mn_{1.94}O_4$ combustion for 6h shows the best capacity retention, the capacity retention rate is 81.25% after 500th cycles, which is better than other samples. It is suggesting that lengthing heat-treating time improved capacity retention of $LiMg_{0.06}Mn_{1.94}O_4$ significantly, because of long reaction time can be improved the stability of the lattice, but when the reaction time to 9h, the capacity retention of $LiMg_{0.06}Mn_{1.94}O_4$ is attenuating. When the crystallinity is good, the diffusion path of lithium ions becomes longer, thus a better crystallity does not mean a good cycle stability.

3.3 Cyclic Voltammetry

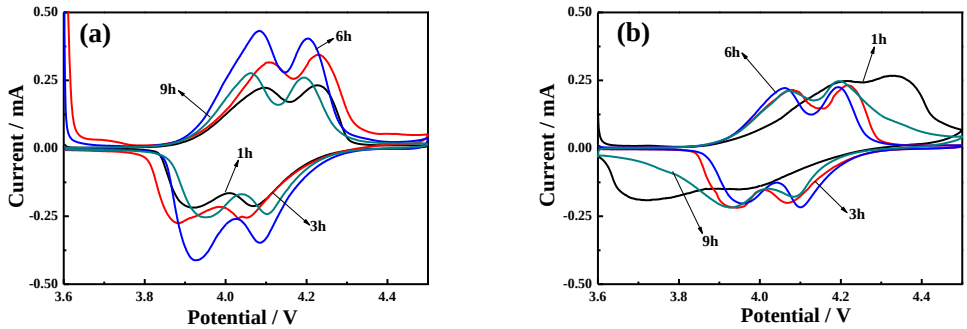

Figure 5. Cyclic voltammogram curves of the $LiMg_{0.06}Mn_{1.94}O_4$ sample synthesized at 500℃ for different time(1h, 3h, 6h and 9h) (a) first time, (b) after 500th cycles

Fig.5(a) present the first cyclic voltammetry of $LiMg_{0.06}Mn_{1.94}O_4$ samples at the scanning rate of 0.05 mV S^{-1}, ranging from 3.6~4.5 V at room temperature. For all of the $LiMg_{0.06}Mn_{1.94}O_4$ samples ,there were two pairs of redox potential peaks around 4.09 V/3.95 V and 4.23 V/4.10 V, which corresponded to the two step reversible (de)intercalation of Li^+ in the spinel phase. It reveals that Mg-doping is not alters the electrochemical mechanism of $LiMn_2O_4$ during cycling[24]. With the increase of combustion reaction time, the cathodic peak potential of $LiMg_{0.06}Mn_{1.94}O_4$ samples have been shift to positive direction, the anodic peak potential have been move to negative direction, the results makes two pairs of redox peak potential difference is becoming smaller and smaller, which was imply that increasing combustion reaction time, can be promote the electrochemical reversibility of the $LiMg_{0.06}Mn_{1.94}O_4$ samples. The Fig.4(b) present the cyclic voltammetry after 500th cycles, it can be clearly find that, The peak area of all samples has been become smaller, which indicated that after 500th cycles, The specific capacity of the material has been reduce. But it can be seen that the peak symmetry of 500℃-6h is still good, indicating that the sample still have good electrochemical reversibility after 500th cycles.

3.4 Calculation of the apparent activation energies

To understand further the electrode kinetics, a series of electrochemical impedance spectroscopies (EIS) were performed at different temperature to calculate the apparent activation energies (E_a) of all samples electrodes, Fig.6(a), (b), (c) and (d) display the Nyquist plots of the electrodes at different temperatures, respectively.

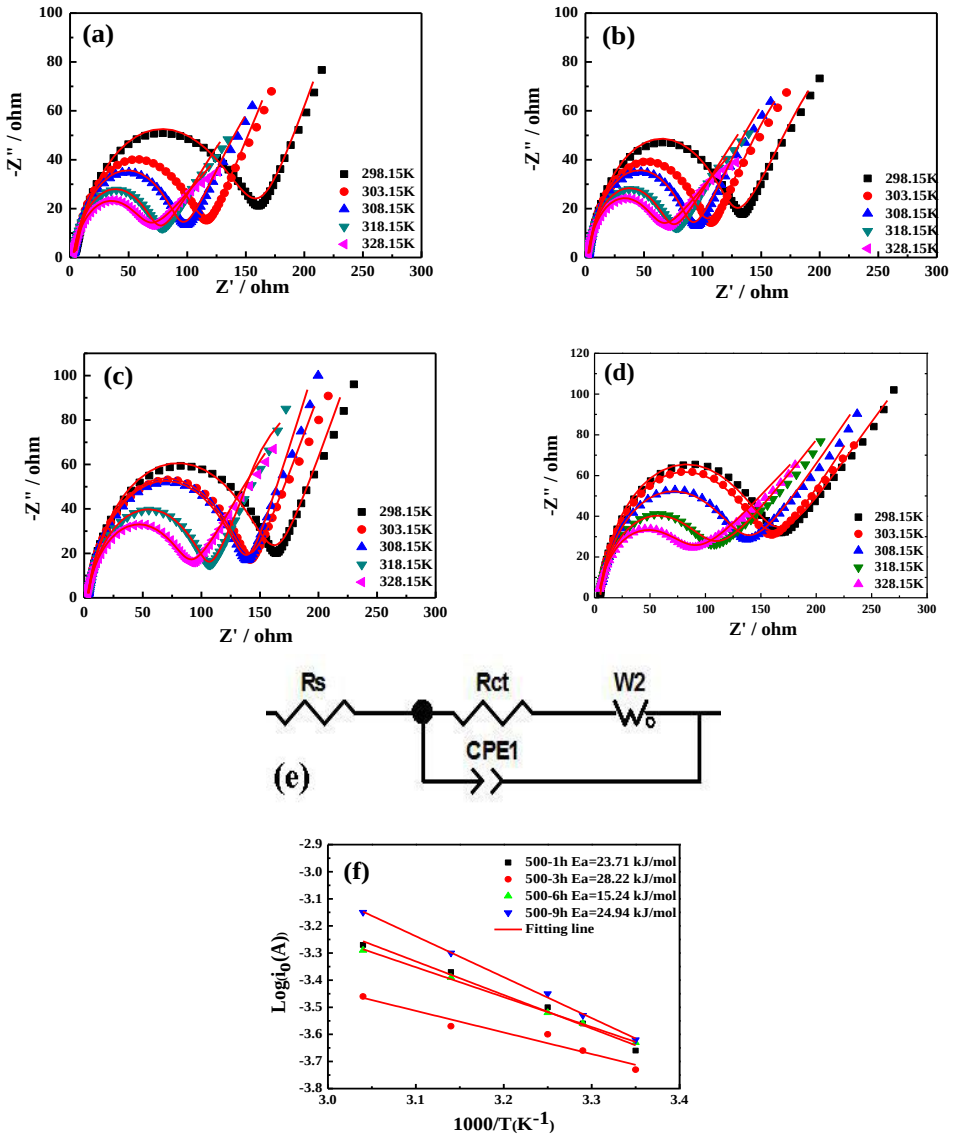

Figure 6. The Nyquist plots of the $LiMg_{0.06}Mn_{1.94}O_4$ samples following different combustion reaction time(a) 1h, (b) 3h, (c) 6h and (d) 9h at different temperatures and (f) Arrhenius plots of log i_0 vs. 1000/T for the electrodes of the $LiMg_{0.06}Mn_{1.94}O_4$ samples at different temperatures

The R_{ct} values can be obtained using the equivalent circuit model shown in Fig.6(e). It can be observed that the R_{ct} values of four electrodes decrease with the increase of temperature. The apparent activation energies (E_a) of all the samples can be determined on the basis of the following equations:

i_0=RT/nFR$_{ct}$ (1)

i_0=Aexp(-E$_a$/RT) (2)

Where i_0 stand for the exchange current, R is the gas constant (8.314 J·mol^{-1}·K^{-1}), T (K) is the absolute temperature, F is the Faraday constant (96484.5 C·mol^{-1})[25]. A is a temperature-independent coefficient, and n is the number of transferred electrons. Arrhenius plots of log i_0 vs. 1000/T for the electrodes of 1, 3, 6 and 9h is exhibited in Fig.6(f). The apparent activation energies (E_a) of all the samples can be calculated to be 23.71. kJ/mol, 28.22 kJ/mol, 15.24 kJ/mol and 24.94 kJ/mol, respectively. Among them, samples obtained at 500℃ for 6h have the smallest apparent activation energy, which is 15.24 kJ/mol, it was indicated that it is more conducive to the dissociation and embedding of Li^+ ions in this condition.

4. CONCLUSIONS

Spinel $LiMg_{0.06}Mn_{1.94}O_4$ were successfully synthesized by a solid-state combustion method. It is using lithium carbonate and manganese carbonate as raw material, magnesium acetate as dopant, and citric acid as fuel. and combustion reaction at 500℃ in different reaction time (1, 3, 6 and 9h). The compounds were characterized by XRD, SEM and XPS. Electrochemical performances were evaluated by cyclic votammetry, EIS, and galvanostatic cycling. As can be seen from the XRD diagram, all as-prepared samples are single phase. With the increasing of reaction time, the crystallinity of $LiMg_{0.06}Mn_{1.94}O_4$ was increased, particle size became bigger, crystal morphology gradually developed to regular octahedrons morphology, and the distribution size of particles became more homogeneous. Among the synthesized materials, the $LiMg_{0.06}Mn_{1.94}O_4$ combustion for 6h exhibited the optimal electrochemical properties, which discharge specific capacities of 101.9 mAh/g, after 500th cycles with capacity retention rate of 81.25%. By Cyclic voltammogram curves can be find that after 500th cycles the sample synthesized by 6h still with a good symmetry. The apparent activation energies (E_a) of all the samples is calculated to be 23.71 kJ/mol, 28.22 kJ/mol, 15.24 kJ/mol and 24.94 kJ/mol, respectively. Among them, samples obtained at 500℃for 6h have the smallest apparent activation energy.

ACKNOWLEDGEMENTS
This work was financially supported by the National Natural Science Foundation of China (51462036, U1602273), and Innovation Program of Yunnan Minzu University (2016YJCXS17).

References

1. H.Y. Zhao, S.S. Liu, Z.W. Wang, M. Tan, C. Yu and X.Q. Liu, *Ceramics International*, 42 (2016) 13442.
2. B. Xu, D.N. Qian, Z.Y. Wang and Y.S. Meng, *Cheminform*, 73 (2012) 51.
3. P.H. Biensan, B. Simon, J.P. Pérès, A.D. Guiberta, M. Brousselyb, J.M. Bodetb and F. Pertonb, J*ournal of Power Sources*, 81–82 (1999) 906.
4. Y.J. Wei, K.B. Kim, G.Chen and C.W. Park, *Materials Characterization*, 59 (2008) 1196.
5. J.W. Fergus, *Journal of Power Sources*, 195 (2010) 939.

6. J.M. Tarascon and M. Armand, *Nature*, 414 (2001) 359.
7. D. Guyomard and J.M. Tarascon, *Solid State Ionics*, 69 (1994) 222.
8. H. Zhang, D. Liu, X.S. Zhang, C.J. Zhao and Y.L. Xu, *Journal of Solid State Electrochemistry*, 18 (2013) 569.
9. M. Prabu, M. Prabu, M.V. Reddy, S. Selvasekarapandian, S. Admas and K.P. Loh, *Journal of the Electrochemical Society*, 160 (2013) A3144.
10. J.L. Wang, Z.H. Li, J. Yang, J.J. Tang, J.J. Yu, W.B. Nie, G.T. Lei and Q.Z. Xiao, *Electrochimica Acta*, 75 (2012) 115.
11. D. Capsoni, M. Bini, G. Chiodelli, V. Massarotti, M.C. Mozzati and C.B. Azzoni, *Solid State Communications*, 125 (2003) 179.
12. R. Thirunakaran, K.T. Kim, Y.M. Kang and J.Y. Lee, *Materials Research Bulletin*, 40 (2005) 177.
13. R. Santhanam and B. Rambabu. *Journal of Power Sources*, 195 (2010) 5442.
14. D. Arumugam, G.P. Kalaignan and P.Manisankar. *Solid State Ionics*, 179 (2008) 580.
15. T.F. Yi, L.C. Yin, Y.Q. Ma, H.Y. Shen, Y.R. Zhu and R.S. Zhu, *Ceramics International*, 39 (2013) 4673.
16. J.J. Huang, F.L. Yang, Y.J. Guo, C.C. Peng, H.L. Bai, J.H. Peng and J.M. Guo, *Ceramics International*, 41 (2015) 9662.
17. M.W. Xiang, L.Q. Ye, C.C. Peng, L. Zhong, H.L. Bai, C.W. Su and J.M. Guo, *Ceramics International*, 40 (2015) 10839.
18. H. Zhang, D. Liu, and X.S. Zhang, *J Solid State Electrochem.*, 18 (2014) 569
19. J.T. Liu, J.B. Hao, J.M. Guo C.W. Su, and R. Wang, *Int. J. Electrochem. Sci.* 11 (2016) 5838
20. B.D. Cullity and S.R. Stock, *Prentice Hall*, 2001, P. 170
21. M.W. Xiang, C.W. Su, L.L. Feng, M.L. Yuan and J.M. Guo, *Electrochimica Acta*, 125 (2014) 524.
22. M. Prabu, M.V. Reddy, S. Selvasekarapandian, G.V. Subba Rao and B.V.R. Chowdari, *Electrochimica Acta*, 88 (2013) 745
23. P. Singh, A. Sil, M. Nath and S. Ray, *Ceram. Silik.*, 54 (2010) 38
24. B.W. Ju, X.Y. Wang, C. Wu, X.K. Yang, H.B. Shu, Y.S. Bai, W.C. Wen and X. Yi, J*ournal of Alloys and Compounds*, 584 (2014) 454
25. S.L. Chou, J.Z. Wang, J.Z. Sun, D. Wexler, M. Forsyth and S.X. Dou, *Chemistry of Materials*, 20 (2010) 7044.